EONS: A Multi-Level Modeling System and Its Applications

Jim-Shih Liaw,[1] Ying Shu,[2] Taraneh Ghaffari,[1] Xiaping Xie,[1] and Theodore W. Berger[1]

[1]*Department of Biomedical Engineering, University of Southern California, Los Angeles, California*
[2]*Department of Computer Science, University of Southern California, Los Angeles, California*

2.3.1 Introduction

A major unresolved issue in neuroscience is how functional capacities of the brain depend on (emerge from) underlying cellular and molecular mechanisms. This issue remains unresolved because of the number and complexity of mechanisms that are known to exist at the cellular and molecular level, their nonlinear nature, and the complex interactions of these processes. Thus, the capability of simulating neural systems at different levels of organization is essential for an understanding of brain function. To this end, we have undertaken the development of a multi-level modeling system, Elementary Objects of Nervous Systems (EONS), to provide a framework for representing structural relationships and functional interactions among different levels of neural organization.

In EONS, object-oriented design methodology is adopted to form a hierarchy of neural models, from molecules, synapses, and neurons to networks. Each model (e.g., for a synapse or a neuron) is self-contained and any reasonable degree of detail can be included. This provides the flexibility to compose complex system models that reflect the hierarchical organization of the brain from objects of basic elements. Our aim is to make EONS objects available for use by models created with other modeling tools. The EONS library is thus separated from the user interface in order to increase its portability.

For computational models to be useful both as interactive research and teaching tools and as means for technology transfer, it is critically important that a closed-loop interaction between computational and experimental studies be provided. This requires a well-structured modeling framework that parallels biological nervous systems and a mechanism for mapping between neurobiological system parameters and model parameters for a direct comparison and interpretation of experimental manipulations and model simulations. To provide a link with experimental studies, we have developed a prototype for protocol-based simulation in which information about a model is organized in the same way as the specifications of an experiment. This prototype has been developed in conjunction with the NeuroCore component of the USC Brain Project focusing on the design of a protocol-based database for experimental data. Together with NeuroCore, NSL (Chapter 2.2), and BMW (Chapter 2.4), EONS will provide an interactive environment for integrating computational and experimental studies.

This chapter is organized into three sections. The EONS object library is presented in the first section, as well as two example models for illustrating the principles and functionalities of EONS. The first example is a detailed model of a synapse that includes the biophysics of the membrane, various channels, and a spatial representation of the synapse for calculating the distribution of particles through the diffusional process. The second example is a neural network that demonstrates how a concise representation of various synaptic processes can be derived from a detailed study for the incorporation of

Copyright © 2001 by Academic Press, Inc.
All rights of reproduction in any form reserved.

synaptic dynamics into neural networks. The second section describes the protocol-based simulation scheme, and the conclusion and future development of EONS are given in the last section.

2.3.2 EONS Object Library

The complexity of the nervous system is enormous due to its vast number of components ranging from molecules, synapses, and neurons to brain regions. Dealing with such complexity calls for a modeling environment that provides a high degree of flexibility for choosing a set of biologically consistent constituents for studying a specific aspect of the brain. Object-oriented methodology provides a flexible scheme for representing the hierarchical organization of the nervous system.

Using object-oriented design methodology, we have developed objects for different neural components, from networks, neurons, dendrites, and synapses down to molecules. Various degrees of detail can be included in any of these objects. An example of a hierarchical representation of a neuron is shown in Fig.1. A neuron can be represented as a simple integrate-and-fire object containing a set of synaptic weights, membrane potential, threshold, and action potential as its attributes. Or, it can be a complex object composed of three objects representing dendrite, soma, and axon; each of these in turn can be a composite of multiple objects. A critical requirement for allowing flexible representation of objects and their composition is a predefined input/output specification, both in terms of its type and semantics. EONS reinforces this by closely following the property of the corresponding biological elements.

For example, one can define a class of neurons that includes a set of dendritic spines and a set of axon terminals. Each neuron receives as input a real number representing the membrane potential of the dendrite and generates a real number representing the membrane potential along the axon. An object representing spine or axon terminals can incorporate any features, as long as it conforms to this I/O specification. For instance, an axon terminal can be represented as a simple relay (identity function) at one end of the spectrum, or it can include various voltage- and ligand-gated channels, calcium diffusion, and the cascade of molecular interactions leading to neurotransmitter release. Likewise, a spine object can be represented simply as a number (synaptic weight), or it can include the kinetics of various receptor channels, etc.

One issue when constructing neural networks models with non-homogeneous elements is finding a way to keep track of the connectivity among these elements. For example, a synaptic element may be comprised of multiple molecular objects (e.g., vesicles, receptor, release site, etc.) which may not be uniformly distributed for each synapse. This precludes the use of convolution, a highly efficient method for updating neural networks used by NSL (Chapter 2.2).

We have developed a systematic indexing scheme to handle such complexity: Given neural networks composed of layers of neurons and the connectivity matrix for each layer, EONS will "grow" the synapses between neurons by automatic generation of bi-directional synap-

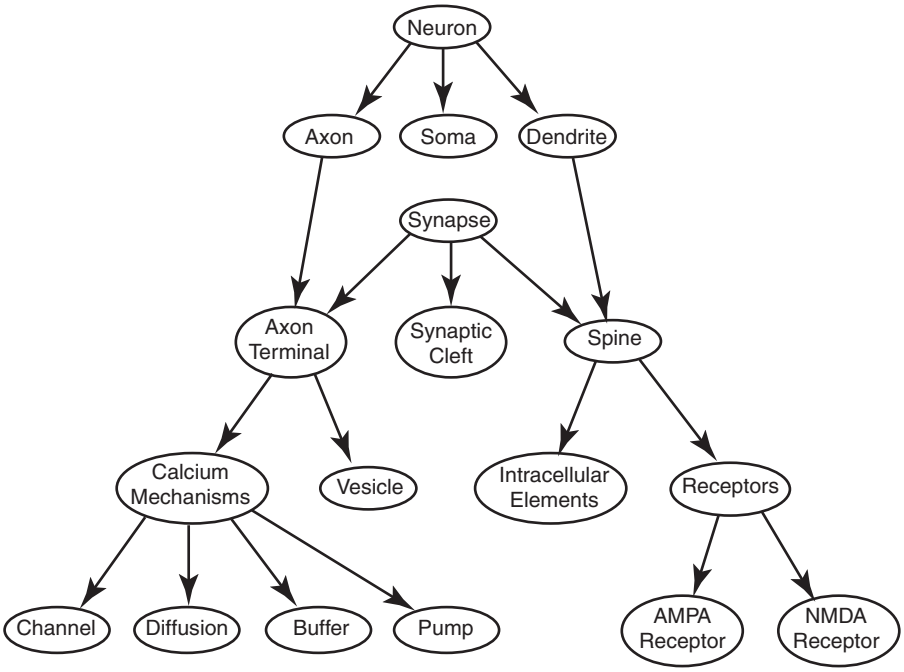

Figure 1 A hierarchy of neuron components.

tic pointers according to the connectivity matrix. This is implemented by the following procedure: From the connectivity matrix, the number of axon terminals and dendritic spines needed for each neuron is counted and instantiated. Next, a bi-directional pointer between each axon terminal and dendritic spine pair, as specified in the connectivity matrix, is set up by going through each neuron in the network.

Moreover, EONS also contains objects representing the network, layers, neurons, axon terminals, and spines. Initially, these objects only contain the specification of the input and output types. These objects, together with the synaptic indexes, form a basic skeleton for building neural models such that various neural processes can be incorporated at each level in a flexible manner. We will illustrate the flexibility of EONS for multi-level model development by the following two examples: a detailed model of a synapse which incorporates morphology revealed by electron microscopy and a dynamic synapse neural network.

A Detailed Model of a Synapse

Synapse, the contact between neurons, is a complex system composed of a multitude of molecular machinery. Typically, it consists of an axon terminal, the end point of the input neuron, and a postsynaptic spine on the dendrite of the second neuron. The axon terminal and the spine is separated by a space called synaptic cleft. Each of the synaptic processes is tightly controlled by a large number of molecular interaction, which themselves are subject to change under a variety of conditions.

To study issues at the synaptic level, we have constructed a model of a glutamatergic synapse which includes three main objects representing the axon terminal, the synaptic cleft, and the postsynaptic spine (Fig. 2A). The basic axon terminal module contains objects of ion channels, calcium mechanisms, vesicle, molecular processes, and intrinsic membrane properties (Fig. 2B). The parameter values that the model used for these objects are based on experimental data and are consistent with those used in many existing models. We have conducted an intensive series of computer simulations of the synaptic model to address a number of unresolved issues regarding synaptic transmission and plasticity (Gaffari *et al.*, 1999; Liaw and Berger, 1999; Xie *et al.*, 1995, 1997). Here, we illustrate a particular extension of this model: the incorporation of morphological details.

Changes in synaptic morphology consistently have been observed as a consequence of a variety of experimental manipulations, including associative learning (Black *et al.*, 1990; Federmeier *et al.*, 1994; Kleim *et al.*, 1994, 1997), environmental rearing conditions (Bhide and Bedi, 1984; Diamond *et al.*, 1964; Globus *et al.*, 1973; Turner and Greenough, 1983, 1985; Volkmar and Greenough, 1972), and increased synaptic "use" induced by direct electrical (Buchs and Muller, 1996; Desmond and Levy, 1983, 1988; Geinisman *et al.*, 1993; Wojtowicz *et al.*, 1989), as well as the processes of normal development and aging (De Groot and Bierman, 1983; Dyson and Jones, 1984; Harris *et al.*, 1992). Some structural changes involve morphological profiles corresponding to "perforated" or "partitioned" synapses. A defining property of perforated and partitioned synapses is the finger-like formations of postsynaptic membrane and cytoplasm enveloped by presynaptic membrane and cytoplasm at single or multiple locations along the synaptic cleft. The pre- and postsynaptic specializations are correspondingly discontinuous, resulting in multiple, compartmentalized synaptic zones within the same end-terminal region.

A model of partitioned synapses was developed to study the impact of structural modifications on neurotransmitter release and synaptic dynamics. Specifically, a

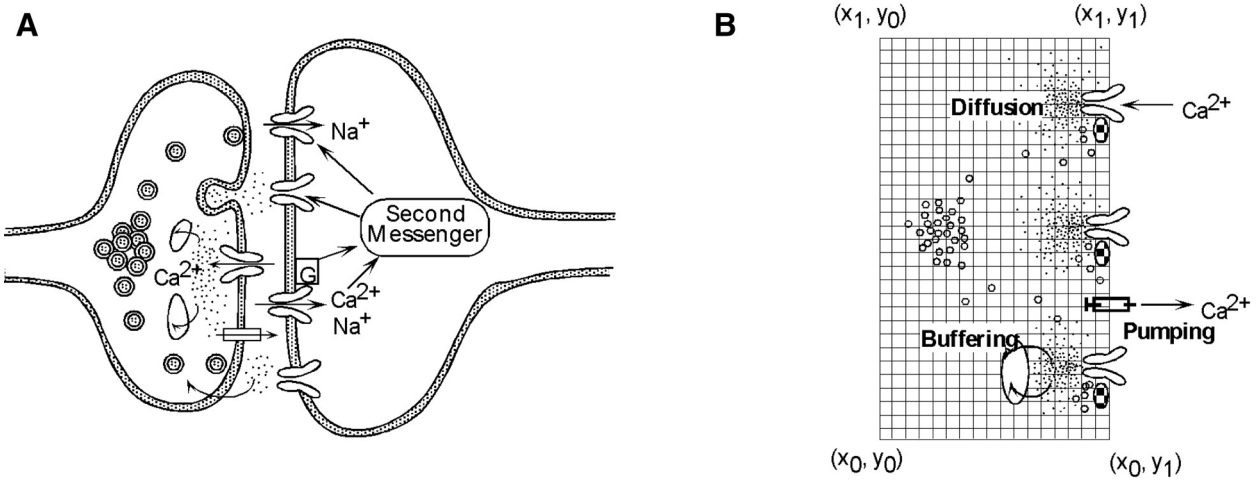

Figure 2 (A) A schematic representation of a synapse. **(B)** A schematic representation of a model of the axon terminal.

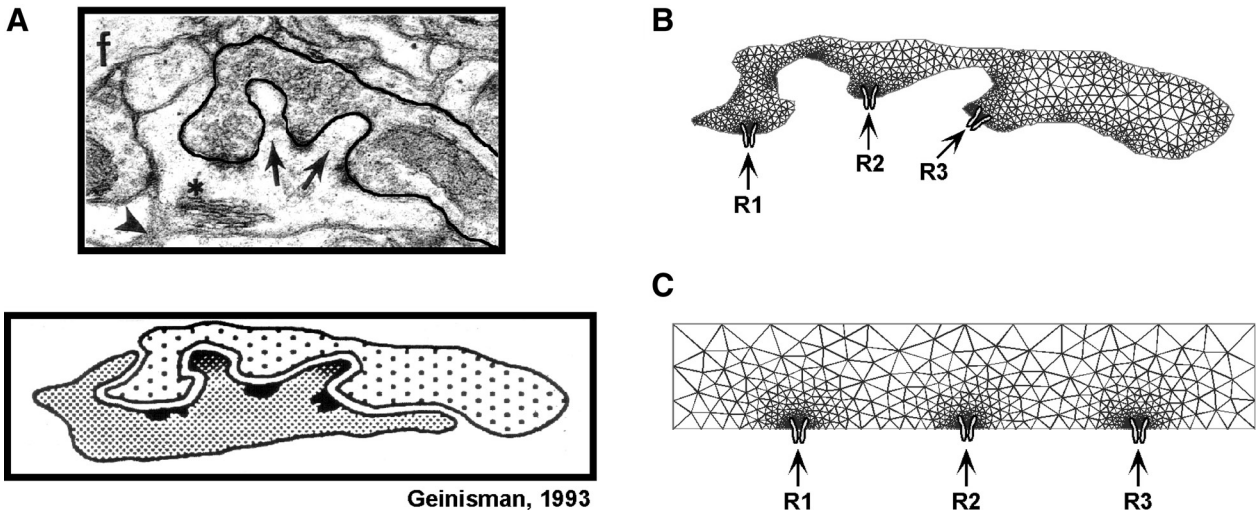

Figure 3 Partitioned synapse: EM data and the model. (From Geinisman *et al.*, 1993. With permission.)

serial section electron micrograph of a hippocampal partitioned synapse (Fig. 3A) after high-frequency stimulation was used to specify the geometry of the model (Fig. 3B).

The general structure of our model of the axon terminal consists of a finite element representation of a two-dimensional geometry, such as that of a partitioned presynaptic terminal. The geometric representation of the model is developed using MATLAB with the "constructive solid geometry" modeling paradigm. The two-dimensional geometry is then discretized by generating a triangular mesh (Fig. 3B). The mesh is refined until the smallest boundary element is just smaller than 0.5 nm wide in order to minimize the approximation error. After the terminal boundary is accurately specified, calcium channels and neurotransmitter release sites are assigned as time-varying boundary conditions. We have extended the mathematical functionality such that boundary conditions can be specified at any location on the boundary. In the case of the partitioned synapse, the calcium channels and release sites are placed (10 nm apart) at positions corresponding to the location of PSDs in the electron micrograph picture. An additional step is taken to refine the mesh such that the triangles near the calcium channels and release sites are higher in number and smaller in size to increase the accuracy of the solution (Fig. 3B). The kinetics of calcium conductance and neurotransmitter release were optimized with experimental data. The diffusion coefficient is specified to include the appropriate rate of calcium buffering. Given the discretized mesh representation of the terminal, the boundary and initial conditions, and the coefficients of the diffusion equation, a numerical solution to the diffusion equation is obtained using the MATLAB partial differential equation toolbox (The MathWorks, 1995).

A series of computer simulations is conducted to test the hypothesis that local structure in the partitioned synapse affects calcium diffusion and distribution and hence the probability of neurotransmitter release. In the first set of simulations, a rectangular model of a symmetrical presynaptic terminal (Fig. 3C) is used as the control for comparison with the partitioned synapse model. There are three equally spaced calcium channel release sites in the control case. Simulations of the symmetrical model show an equal release probability for all of the release sites for both a single depolarization step and a train of random inputs (i.e., a sequence of depolarization steps over 200 msec, shown in Fig. 4B).

Simulations of the partitioned synapse model (see Fig. 3B) in response to a single depolarization step show that the probability of release is different for the three release sites. The peak amplitude of release probability for site 1 is 32% higher than that of site 2 and 19% higher than that of site 3 (Fig. 4A). The results indicate that the differences in the release probability within the time course of a single response are a consequence of unequal morphological partitioning. Next, we simulate the partitioned synapse model with the random train of inputs. The peak response of site 1 to a sequence of depolarization steps (Fig. 4B) varied with respect to site 3. For example, the peak response of site 3 was higher than that of site 1 in response to the group of six consecutive pulses beginning with the second pulse (at 15 msec). However, the relative peak amplitudes of the two sites reversed from the eighth pulse to the end of the input train, revealing different temporal dynamics within a single synapse.

A series of computer simulations was conducted to test the hypothesis that morphological alterations lead to variations in synaptic dynamics by systematically examining a variety of spatial features. For instance, the effect of a nearby membrane wall was examined by moving release site 3 in the partitioned synapse approximately 300 nm to the right (Fig. 5). The reversal in the relative

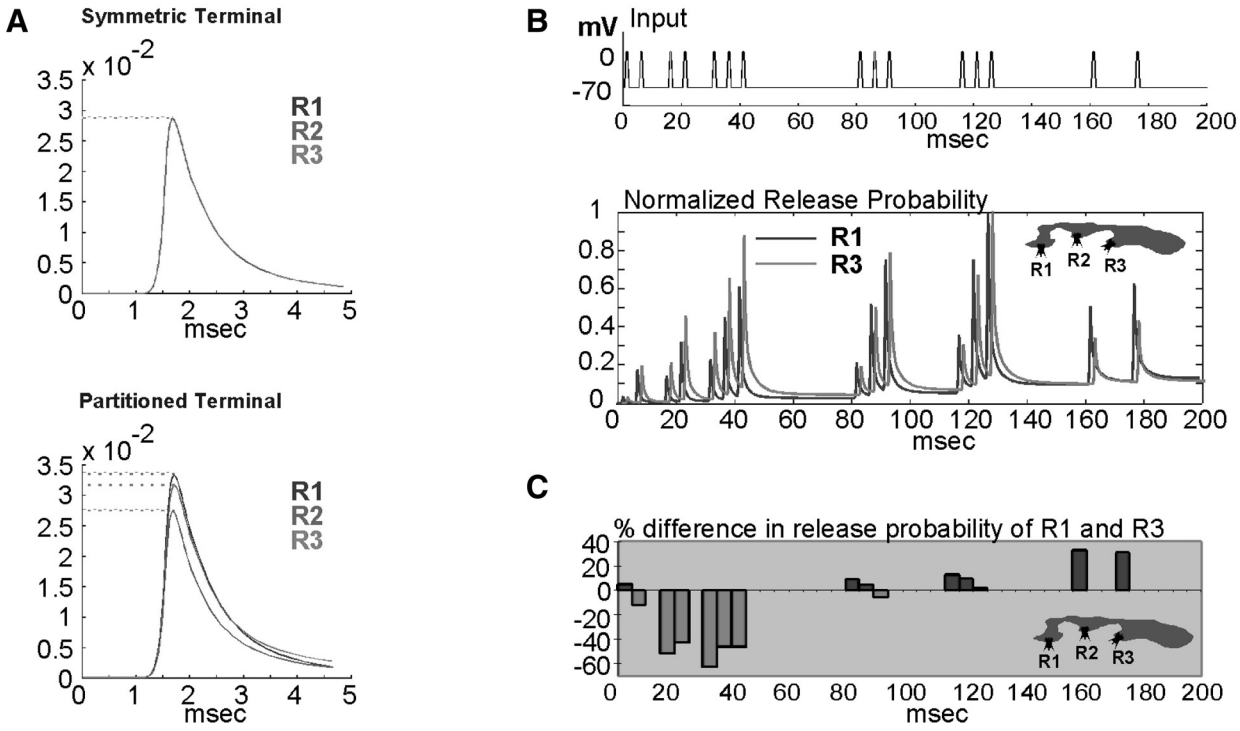

Figure 4 Release probability in the symmetric terminal and the partitioned synapse.

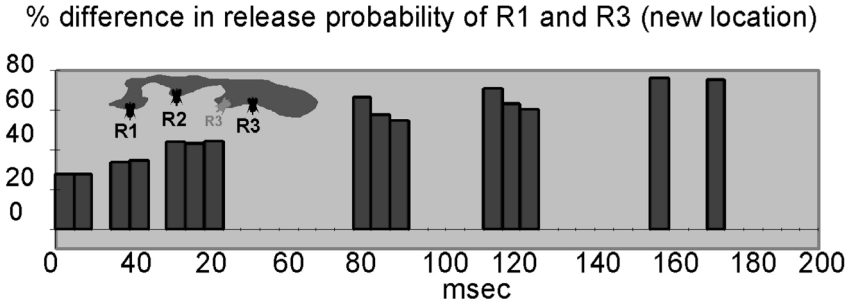

Figure 5 Effect of proximity to adjacent membrane wall on release probability.

peak amplitudes between release sites 1 and 3 seen in Fig. 4 is eliminated. Instead, the probability of release is always higher in release site 1 than release site 3 at the new location.

Dynamic Synapse Model

In the previous section, we presented a detailed model of a glutamatergic synapse. Though such a comprehensive model of a synapse is necessary for studying synaptic transmission, its complexity precludes the details being carried over to a neural network of any significant size. Instead, one must extract essential principles of the synaptic processes, which can be gained only through a careful and in-depth study of that particular level, to provide proper abstraction and simplification necessary not only for the feasibility of modeling, but also, more importantly, for insight regarding the emergence of higher level functionalities from cellular or molecular mechanisms.

Here we show one example, the development of the concept of the *dynamic synapse*, which captures the essential principles of neurotransmitter release with only a few equations. This concise mathematical representation is extracted from simulations of the detailed synaptic models described in the previous section. With the systematic indexing scheme of EONS, we have constructed a neural network model incorporating dynamic synapses which is used to perform the task of speech recognition.

A straightforward implementation of the dynamic synapse is by expressing the potential of neurotransmitter release as a weighted sum of the activation of presynaptic mechanisms:

$$R_i(t) = \sum_m K_{i,m}(t) F_{i,m}(Ap(t)) \quad (1)$$

where $R_i(t)$ is the potential for release for presynaptic terminal $i$at time t. $F_{i,m}$ is the m'th mechanism in terminal i, $K_{i,m}$ is the coefficient (weight) for mechanism $F_{i,m}$, and Ap indicates the occurrence ($Ap = 1$) or non-occurrence ($Ap = 0$) of an action potential. Any number of synaptic mechanisms (e.g., facilitation, augmentation, PTP, modulation, etc.) can be included in this equation. Note that in this implementation, R is deterministic, though it can be made stochastic by, say, expressing it as a probability variable and adjusting all the other parameters to be consistent with the probability constraints (e.g., probability of release ≤ 1).

One simple expression, known as the leaky-integrator equation, can be used to describe the dynamics of various synaptic mechanisms:

$$\tau_{i,\,m} \frac{dF_{i,\,m}(t)}{dt} = -F_{i,\,m}(t) + Ap(t) \quad (2)$$

where $\tau_{i,m}$ is the time constant of mechanism m in terminal i. Other equations can also be used to express synaptic mechanisms, such as the alpha function, without deviation from the spirit of a dynamic synapse. Typically, $F_{i,m}$ is a function of the presynaptic action potential, $Ap(t)$. That is, the magnitude of Fi,m varies continuously based on the temporal pattern of the spike train. Usually, $Ap(t)$ originates from the same neuron that gives rise to the particular axon terminal; however, $Ap(t)$ may also be the action potential generated by some other neuron, such as the case of feedback modulation. Furthermore, $F_{i,m}$ can also be a function of other type of signals. For example, it can be a function of the synaptic signal generated by the same axon terminal i (e.g., via presynaptic receptor channels) or a function of the synaptic signals produced by other synapses (e.g., via axon-axonal synapses).

A quanta of neurotransmitter is released if R is greater than a threshold (θR) and there is at least one quanta of neurotransmitter available (N_{total}):

$$\text{If}(\mathrm{P_R} > \theta_\mathrm{R} \;\&\; \mathrm{N_{total}Q}) \text{ then } \mathrm{N_R} = \mathrm{Q} \text{ and } \mathrm{N_{total}} = \mathrm{N_{total}} - \mathrm{Q}. \quad (3)$$

where N_R is the concentration of neurotransmitter in the synaptic cleft. Note that the reduction of available neurotransmitter represents an underlying cause of synaptic depression. The neurotransmitter is cleared from the synaptic cleft at an exponential rate with time constant τ_{N_t}:

$$N_R = N_{R^e}^{-t/\tau_{N_t}} \quad (4)$$

Furthermore, there is a continuous process for replenishing neurotransmitter:

$$\frac{dN_{total}}{dt} = \tau_{rp}(N_{\max} - N_{total}) \quad (5)$$

where $N_{\max}$ is the maximum amount of available neurotransmitter and τ_{rp} is the rate of replenishing neurotransmitter.

The postsynaptic potential (PSP) is a function (G) of the concentration of the neurotransmitter in the synaptic cleft:

$$PSP_j(t) = \sum_n W_{j,n}(t)^* G_{j,n}(N_i(t)) \quad (6)$$

where $W_{j,n}$ denotes the efficacy of mechanism n at the postsynaptic site j to respond to signals from presynaptic terminal i. Typical postsynaptic mechanisms are conductances generated by various types of receptor channels. They can be expressed in a way similar to presynaptic mechanisms (e.g., Eq. (2) or the alpha function). Different kinetics of receptor channels can be approximated by adjusting the time constants in Eq. (2) (or the alpha function).

The postsynaptic potentials can be integrated at the soma of an "integrate-and-fire" model neuron:

$$\tau_v \frac{dV(t)}{dt} = -V(t) + \sum_s PSP_s(t) \quad (7)$$

where V is the somatic membrane potential and τ_v is the time constant. An action potential is generated (i.e., $Ap = 1$) if V crosses some threshold.

Dynamic Learning Algorithm

The process of neurotransmitter release is dynamically mediated by complex molecular and cellular mechanisms. Furthermore, these mechanisms themselves are dynamic and under constant regulation and modulation. How can such second-order regulation be expressed mathematically? An even more intriguing question is how can such regulation be utilized for learning and memory? One plausible answer is to modify the presynaptic mechanisms by the correlation of presynaptic and postsynaptic activation. The biological plausibility is based on the existence of molecules that are attached to both pre- and post-synaptic membranes (e.g., those that are thought to bind the two membranes together). These molecules can provide a means for conveying the activation signal of the postsynaptic neuron to the presynaptic terminal. The theoretical plausibility is rooted in the notion of the Hebbian rule. More specifically, the contribution of each synaptic mechanism to the release of neurotransmitter or the activation of postsynaptic potentials is changed as shown below:

$$\Delta K_{M,i} = \alpha_M * L_{M,i} * Ap_j \quad (8)$$

where $K_{M,i}$ is the co-efficient of synaptic mechanism M in synapse i, αM is the learning rate for M, $L_{M,i}$ is the activation level of M in synapse i, and Ap_j (= 0 or 1) indicates the occurrence or non-occurrence of an action

potential of postsynaptic neuron j. Note that the mechanisms in Eq. (8) also include those in the postsynaptic site, which is equivalent to the conventional Hebbian rule for changing "synaptic efficacy" or "synaptic weight."

By changing the contribution of each synaptic mechanism to the process of neurotransmitter release, the transformation function of the axon terminal is modified. And, by basing such changes on the correlation of pre- and postsynaptic activation, an axon terminal can learn to extract temporal patterns of action potential sequences that occur consistently. That is, each axon terminal will extract different statistical regularities (invariant features) embedded in the spike train, whereas correlated changes in the postsynaptic mechanisms (i.e., the synaptic efficacy or weight) determine how such presynaptic signals should be combined.

Speech Recognition Case Study

We have demonstrated the computational capability of dynamic synapses by performing speech recognition from unprocessed, noisy raw waveforms of words spoken by multiple speakers with a simple neural network consisting of a small number of neurons connected by dynamic synapses (Liaw and Berger, 1996, 1999). The neural network is organized into two layers, an input layer and an output layer, with five neurons in each layer, plus one inhibitory interneuron, each modeled as an "integrate-and-fire" neuron (Fig. 6). The input neurons receive unprocessed, raw speech waveforms. Each input neuron is connected by dynamic synapses to all of the output neurons and to the interneuron, with a total of $5 \times 6 = 30$ dynamic synapses in the model. There is a feedback connection from the interneuron to each presynaptic terminal providing the inhibition. We experimented with two learning procedures for this small neural network.

The first experiment involved unsupervised learning. Given a set of N words spoken by M speakers, the goal is to train the neural network to converge to N distinct output patterns at the output neurons. The network is trained following Hebbian and anti-Hebbian rules. During learning, the presentation of the raw speech waveforms is grouped into blocks in which the waveforms of the same word spoken by different speakers are presented to the network a total of 20 times. Within a presentation block, the Hebbian rule is applied. In this way, the responses to the temporal features that are common in the waveforms will be enhanced, while the idiosyncratic features will be discouraged. When the presentation first switches to the next block of waveforms of a new word, the anti-Hebbian rule is applied. This enhances the differences between the response to the current word and the response to the previous, different word. As the learning process progresses, the output patterns of neural network gradually converges to N distinct clusters, each corresponding to a given word. Our dynamic synapse neural network has successfully generated invariant output patterns for $N = 12$ different words (readers are referred to Liaw and Berger, 1996, 1999, for more details).

The second experiment applied supervised learning to making use of the invariant features obtained in experiment 1 to achieve word recognition by forcing each output neuron to respond preferentially to a specific word. The results demonstrated that, by making use of the set of invariant features that were extracted dynamically during unsupervised training, the network can readily perform word recognition. We then tested the robustness of our model when the speech signals are corrupted with progressively increasing amount of noise. The results showed that our model is extremely robust against noise, retaining an 85% performance rate with SNR $= -30$ when the recognition threshold is dynamically adjusted. This performance is better than human listeners tested with the same speech data set.

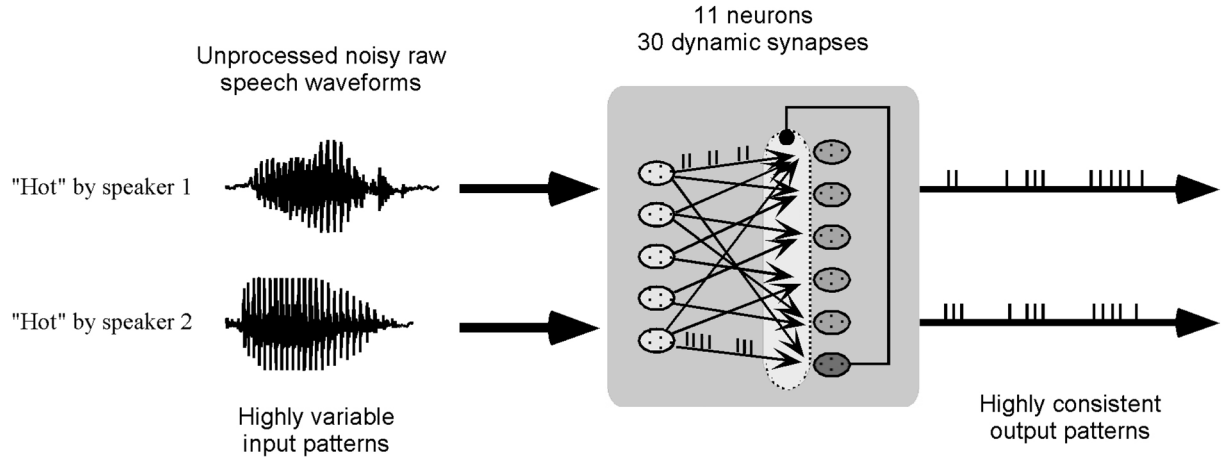

Figure 6 A dynamic synapse neural network model for speech recognition.

2.3.3 Protocol-Based Simulation

A tight coupling with experimental studies is critically important for the success of a computational model. This is particularly important given that experimental and computational approaches can complement each other. For example, it is difficult, if not impossible, to physically translocate certain molecules in a biological neuron with current experimental methods. This can be easily achieved with a computational model with an appropriate spatial representation. On the other hand, it is very difficult to solve the diffusion equation over a complex three-dimensional space, a process that can readily be manipulated experimentally. To increase the synergy between empirical and computational neuroscience, a communication language for these two disciplines is needed. One of the fundamental characteristics of biological experiments is the testing of certain hypotheses. The experimental procedures for testing a hypothesis can be fully characterized by a set of protocols that specify the conditions of the experiment and the manipulations of system parameters. Correspondingly, we have developed a protocol-based simulation scheme to facilitate the communication between these two disciplines.

Furthermore, one of the major difficulties in integrating the experimental and modeling approaches is finding relevant data to constrain model parameters such that comparisons of the simulation results and experimental data can be grounded. Currently, the search for relevant data has been done manually in an *ad hoc* manner. The protocol-based simulation scheme can establish a link to experimental databases to alleviate the data searching problem. We will illustrate this simulation scheme using a case study of the formulation and testing of a specific hypothesis that receptor channel aggregation on the postsynaptic membrane is the cellular mechanism underlying the expression of long-term potentiation (Xie *et al.*, 1997).

In the protocol-based scheme, information of a simulation is organized into two levels, namely, a meta level which spells out the hypothesis being tested and a procedural level which contains initial conditions and manipulations of model parameters. The formal specification of a simulation manipulation is given below:

Definition: Let simulation manipulation = [*T, P*], where

$T = [(T_{1,1}, T_{1,2}, \ldots T_{1,n}); \quad (T_{2,1}, T_{2,2}, \ldots T_{2,m}); \quad \ldots (T_{k,1}, T_{k,2}, \quad \ldots T_{k,t})]$. $P = [(P_x, V_{1,1}, V_{1,2}, \quad \ldots, V_{1,n}); (P_y, V_{2,1}, V_{2,2}, \ldots V_{2,m}) \ldots (P_z, V_{k,1}, V_{k,2}, \ldots V_{k,t}]$.

T is a list of points in time where corresponding particular parameter manipulations take place. P is a list of manipulations applied to model parameters during the period T. For example, $(T_{1,1}, T_{1,2}, \ldots)$ together with $(P_x, V_{1,1}, V_{1,2}, \ldots)$ specify that parameter P_x in a simulation is changed from initial value to $V_{1,1}$ at time $T_{1,1}$ and to $V_{1,2}$ at time $T_{1,2}$, and so forth.

Model parameters are grouped into two classes, namely, *conditions*, which include those parameters that remain constant throughout the simulation, and *manipulations*, which contain the time-stamped changes of parameters as defined above. Many default values can be used in the condition part to simplify the specification process. A series of simulations to test a specific hypothesis is organized into blocks, with each block consisting of multiple trials. Manipulations that remain constant for all trials in a block are specified once at the block level, whereas those that vary from trial to trial are specified on a trial-basis. This simulation organization closely matches the structure of an experimental protocol in NeuroCore. We illustrate the protocol-based simulation scheme by the following example of using the synaptic model mentioned in the previous section to study molecular/cellular mechanisms underlying long-term potentiation (LTP).

Simulation Protocols for Testing Alternative Hypotheses of LTP

Long-term potentiation (LTP) is a widely studied form of use-dependent synaptic plasticity expressed robustly by glutamatergic synapses of the hippocampus. Although there is a convergence of evidence concerning the cellular/molecular mechanisms mediating the induction of NMDA receptor-dependent LTP, there remains substantial debate as to the underlying molecular/cellular mechanisms. Here, we illustrate three hypotheses regarding possible mechanisms and the corresponding simulation protocols for testing these hypotheses.

The key data set for testing alternative hypotheses is provided by the experimental component of USCBP (electrophysiological experiment conducted by Xie in Berger's lab; see Xie *et al.*, 1997). The main finding of the experiment is that during the initial phase of LTP, AMPA receptor-mediated responses evoked by presynaptic stimulation are increased; however, AMPA responses to focal application of agonist are not affected.

The following simulation protocols for testing alternative hypotheses use a synaptic cleft object and a kinetic model object from the EONS library (Fig. 1). The synaptic cleft object contains a spatial representation of the space between the pre-and postsynaptic membranes as a two-dimensional array (20 nm wide by 1000 nm long; Fig. 7A). The PDE method in the EONS library is applied to solve the diffusion of neurotransmitter in the synaptic cleft. The object contains a simple kinetic scheme:

$$A + B = \underset{K_{-1}}{\overset{K_1}{\rightleftharpoons}} AB \underset{K_{-2}}{\overset{K_2}{\rightleftharpoons}} AB^*$$

where A represents the concentration of neurotransmitter at the position where the receptor B is located on the postsynaptic membrane, AB represents the probability that B is bound to the neurotransmitter, and AB^* repre-

sents the probability that B is bound and open. K_1, K_{-1}, K_2, and K_{-2} are the binding, unbinding, opening, and closing rates, respectively. The amplitude of excitatory postsynaptic potential (EPSP) is proportional to AB^*.

The following simulation protocols demonstrate how the above synaptic model can be used to test alternative hypotheses regarding mechanisms underlying LTP.

Hypothesis 1: An increase in the neurotransmitter release is the underlying mechanism.

The corresponding simulation protocol is constructed by varying the concentration of agonist, A, across different trials (see Table 1).

Table 1

Trial #1	$[T_{1,1}, T_{1,2}, T_{1,3}); (A, 0, 100, 0)]$
Trial #2	$[T_{1,1}, T_{1,2}, T_{1,3}; (A, 0, 200, 0)]$
Trial#3	$[(T_{1,1}, T_{1,2}, T_{1,3}); (A, 0, 400, 0)]$

Hypothesis 2: Changes in binding rate constant (K_1) are the basis for synaptic plasticity.

The corresponding simulation protocol is similar to that for testing Hypothesis 1 except that the binding rate constant, K_1, is varied across trials (see Table 2).

Table 2

Trial #1	$K_1 = 0.1$
Trial #2	$K_1 = 0.2$
Trial #3	$K_1 = 0.4$

Hypothesis 3: Changes in the distribution of receptor (B) are the mechanisms underlying synaptic plasticity.

The key component of the protocol is the variation of the location of the receptor channel, B, from trial to trial (see Table 3).

Table 3

Trial #1	Loc-of-$B = 0$ nm from release site
Trial #2	Loc-of-$B = 20$ nm from release site
Trial #3	Loc-of-$B = 40$ nm from release site

The Results of Three Simulation Protocols

For each simulation, the perfusion of neurotransmitter (A) into the synapse is simulated by allowing glutamate to diffuse into the synaptic cleft from the edges. The time-evolution of A is calculated by solving the diffusion equation. The results from the three simulation protocols are given below.

PROTOCOL 1

The simulation result based on this protocol showed that the magnitude of EPSC is higher when the amount of agonist is increased. This is inconsistent with the experimental data described above showing that when agonist is directly applied AMPA response does not show an increase after LTP induction.

PROTOCOL 2

The simulation result based on this protocol showed that the magnitude of EPSC is higher when the binding rate is increased. This is inconsistent with the experimental data described above.

PROTOCOL 3

The simulation result based on this protocol showed that the magnitude of EPSC is similar when the receptor (B) is located in different places. This is due to the uniform distribution of agonist throughout the synaptic cleft after perfusion, making the difference in receptor location irrelevant. The simulation result is consistent with the experimental data.

In an additional block of trials, the above simulation condition is changed slightly such that the neurotransmitter is released from a specific presynaptic release site. Under this condition, the simulations show that the resulting EPSC is 42% larger in magnitude when the release site and receptors are in complete alignment with the release site (i.e., Loc-of-$B = 0$ nm) compared to the EPSCs simulated when B is located 40 nm away (Fig. 7B and C). Furthermore, the rising and decaying phases of the EPSC become faster, in agreement with experimental data (further examination revealed that the receptor is bound at the 40 nm location with a probability of 0.23; therefore, a higher probability for receptor binding can be achieved when the receptor moves closer to the release site). The results suggest that hypothesis 3 is the most likely candidate for explaining the molecular/cellular mechanisms underlying LTP. Thus, by constructing a model that includes appropriate representation of the synapse and a protocol for mapping experimental data and model simulation, one can formulate multiple biologically based hypotheses and identify the one that is most consistent with experimental observations.

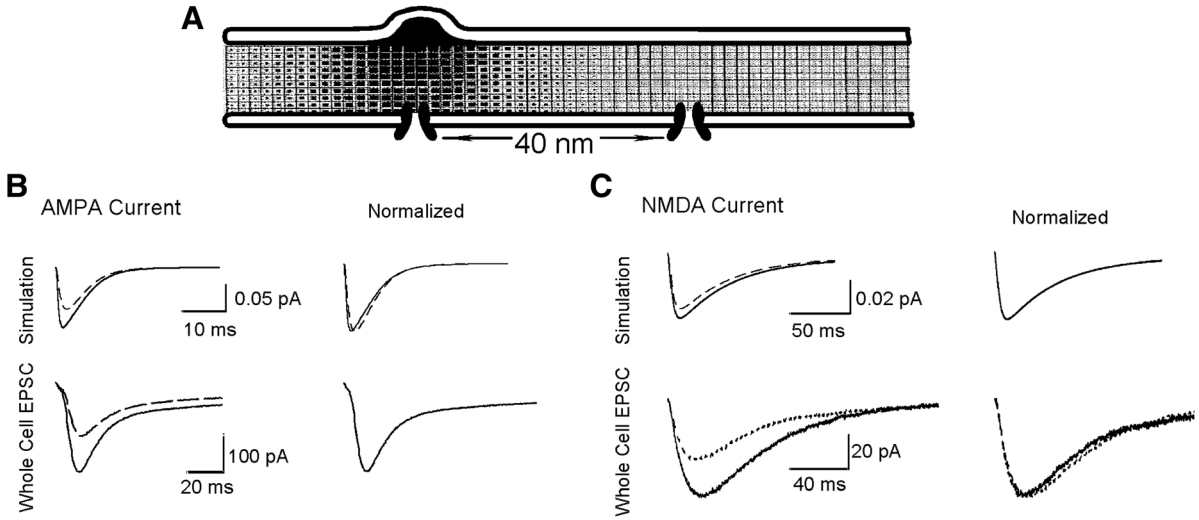

Figure 7 **(A)** A model that includes representations of synaptic cleft and postsynaptic receptors. Comparisons of simulation results with experimental data are provided in **(B)** and **(C)**.

2.3.4 Conclusion

This chapter has provided an introduction to the multi-level modeling system, EONS. In EONS, object-oriented design methodology is employed to facilitate the construction of a hierarchy of neural models ranging from cellular mechanisms, synapses, and neurons to networks. Each model (e.g., for a synapse or a neuron) is self-contained, and various degrees of detail can be included. This provides a way to compose complex system models from objects of basic elements. One objective is to make EONS objects available for use by models created with other modeling tools. For this purpose, the EONS library is separated from the user interface to increase its portability. Two examples were presented; one is a detailed model of a synapse in the hippocampus with complex geometry, and the other is a neural network incorporating dynamic synapses.

Currently, the EONS library contains objects for voltage-gated ion channels; receptor channels; kinetics of molecular interaction; synaptic models; dynamic synapses, neurons, and neural networks; and methods for building complex two-dimensional geometry and solving diffusion over such geometry. Though these objects can be combined to build more complex models, at the present this task has to be carried out manually. One future development plan involves using the Schema Capture System of NSL (Chapter 2.2) to provide a graphic user interface for object composition.

In order to enhance the communication between modelers and experimentalists, we are developing protocol-based simulation for people in the two disciplines to interact with each other more easily. The simulation protocols closely match the structure of an experimental protocol in NeuroCore. One advantage of using similar protocols for both experiments and model simulation is to help make explicit the assumptions adopted in developing the model. Furthermore, queries for searching experimental databases can be adapted for retrieving models stored in databases. Future developments will aim at providing a mechanism for composing models with proper objects based on the specifications derived from a user-defined simulation protocol.

Acknowledgments

This research was supported by the University of California Human Brain Project (with funding from NIMH, NASA, and NIDA), NIMH (MH51722 and MH00343), NCRR Biomedical Simulations Resource (P41 RR01861), ONR (N00014-98-1-0259), and the Human Frontiers Science Organization.

References

Bhide, P. G., and Bedi, K. S. (1984). The effects of a lengthy period of environmental diversity on well-fed and previously undernourished rats. II. Synapse-to-neuron ratios. *J. Comp. Neurol.* **227**, 305–310.

Black, J. E., Isaacs, K. R., Anderson, B. J., Alcantara, A. A., and Greenough, W. T. (1990). Learning causes synaptogenesis, whereas motor activity causes angiogenesis, in cerebellar cortex of adult rats. *Proc. Nat. Acad. Sci. USA*. **87**, 5568–72.

Buchs, P. A., and Muller, D. (1996). Induction of long-term potentiation is associated with major ultrastructural changes of activated synapses. *Proc. Nat. Acad. Sci. USA*. **93**, 8040–8045.

De Groot, D. M., and Bierman, E. P. (1983). The complex-shaped "perforated" synapse, a problem in quantitative stereology of the brain. *J. Microsc.* **131**, 355–360.

Desmond, N. L., and Levy, W. B. (1983). Synaptic correlates of associative potentiation/depression: an ultrastructural study in the hippocampus. *Brain Res.* **265**, 21–30.

Desmond, N. L., and Levy, W. B. (1988). Synaptic interface surface area increases with long-term potentiation in the hippocampal dentate gyrus. *Brain Res.* **453**, 308–314.

Diamond, M. C., Krech, D., and Rosenzweig, M. R. (1964). The effects of an enriched environment on the histology of the rat cerebral cortex. *J. Comp. Neurol.* **123**, 111–120.

Dyson, S. E., and Jones, D. G. (1984). Synaptic remodelling during development and maturation: junction differentiation and splitting as a mechanism for modifying connectivity. *Brain Res.* **315**, 125–137.

Federmeier, K., Kleim, J. A., Anderson, B. J., and Greenough, W. T. (1994). Formation of double synapses in the cerebellar cortex of the rat following motor learning. *Soc. Neurosci. Abstr.* **20**, 1435.

Gaffari, T., Liaw, J.-S., and Berger, T. W., (1999). Consequence of morphological alterations on synaptic function. *Neurocomputing*. **26/27**, 17–27.

Geinisman, Y., de Toledo-Morrell, L., Morrell, F., Heller, R. E., Rossi, M., and Parshall, R. F. (1993). Structural synaptic correlate of long-term potentiation: formation of axospinous synapses with multiple, completely partitioned transmission zones. *Hippocampus*. **3**, 435–446

Globus, A., Rosenzweig, M. R., Bennett, E. L., and Diamond, M. C. (1973). Effects of differential experience on dendritic spine counts in rat cerebral cortex. *J. Comp. Physiol. Psychol.* **82**, 175–181.

Harris, K. M., Jensen, F. E., and Tsao, B. (1992). 3-dimensional structure of dendritic spines and synapses in rat hippocampus at postnatal day-15 and adult ages: implications for the maturation of synaptic physiology and long-term potentiation. *J. Neurosci.* **12**, 2685–2705.

Kleim, J. A., Napper, R. M. A., Swain, R. A., Armstrong, K. E., Jones, T. A., and Greenough, W. T. (1994). Selective synaptic plasticity in the cerebellar cortex of the rat following complex motor learning. *Soc. Neurosci. Abstr.* **20**,1435.

Kleim, J. A., Vij, K., Ballard, D. H., and Greenough, W. T. (1997). Learning-dependent synaptic modifications in the cerebellar cortex of the adult rat persist for at least 4 weeks. *J. Neurosci.* **17**, 717–721.

Liaw, J.-S., and Berger, T. W. (1996). Dynamic synapse: a new concept of neural representation and computation. *Hippocampus*. **6**, 591–600.

Liaw, J.-S., and Berger, T. W. (1999). Dynamic synapse: harnessing the computing power of synaptic dynamics. *Neurocomputing* **26/27**, 199–206.

Shu, Y., Xie. X., Liaw, J.-S., and Berger, T. W. (1999). A protocol-based simulation for linking computational and experimental studies. *Neurocomputing* **26/27**, 1039–1047.

Turner, A. M., and Greenough, W. T. (1983). Synapses per neuron and synaptic dimensions in occipital cortex of rats reared in complex, social or isolation housing. *Acta Stereol. (Suppl.)* **2**, 239–244.

Turner, A. M., and Greenough, W. T. (1985). Differential rearing effects on rat visual cortex synapses. I. Synaptic and neuronal density and synapses per neuron. *Brain Res.* **329**, 195–203.

Volkmar, F. R., and Greenough, W. T. (1972). Rearing complexity affects branching of dendrites in the visual cortex of the rat. *Science* **176**, 1145–1147.

Wojtowicz, J. M., Marin, L., and Atwood, H. L. (1989). Synaptic restructuring during long-term facilitation at the crayfish neuromuscular junction. *Can. J. Physiol. Pharmacol.* **67**, 167–171.

Xie, X., Liaw, J.-S., Baudry, M., and Berger, T. W. (1995). Experimental and modeling studies demonstrate a novel expression mechanism for early phase of long-term potentiation. *Computational Neural Syst.* 33–38.

Xie, X., Liaw, J.-S., Baudry, M., and Berger, T. W. (1997). Novel expression mechanisms for synaptic potentiation: alignment of presynaptic release site and postsynaptic receptor. *Proc. Nat. Acad. Sci. USA*. **94**, 6983–6988.